BRIGHAM HEALTH

BRIGHAM AND WOMEN'S HOSPITAL

Imaging Advances in Smoking-related Injury: From COPD to Interstitial Lung Disease

Raúl San José Estépar, PhD

Applied Chest Imaging Laboratory

Brigham and Women's Hospital

HARVARD MEDICAL SCHOOL TEACHING HOSPITAL

A FOUNDING MEMBER OF PARTNERS HEALTHCARE

Quantitative Imaging Workshop, XV

Smoking Related Lung Disease

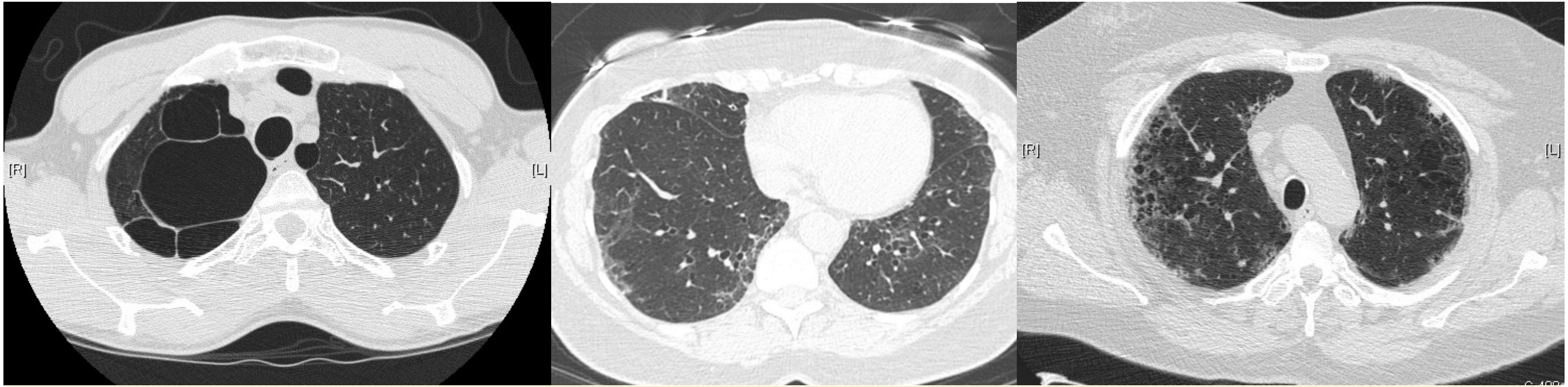

Emphysema/COPD ⟷ Overlap ⟷ Pulmonary Fibrosis

Designing Imaging Phenotypes: Computational Imaging

Endotype

Histopathology / Structural Changes

Imaging Phenotype

Hypotheses

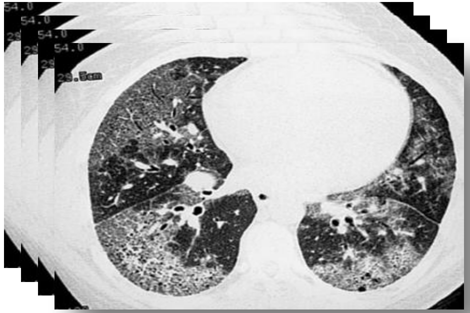

Computational Imaging

Endophenotype

Diagnosis
Prediction
Monitoring

What are the *imaging endophenotypes* that are linked to the clinical manifestation and the prognostication of smoking related injury and *poor lung development*?

Emphysema Subtyping via Local Histogram

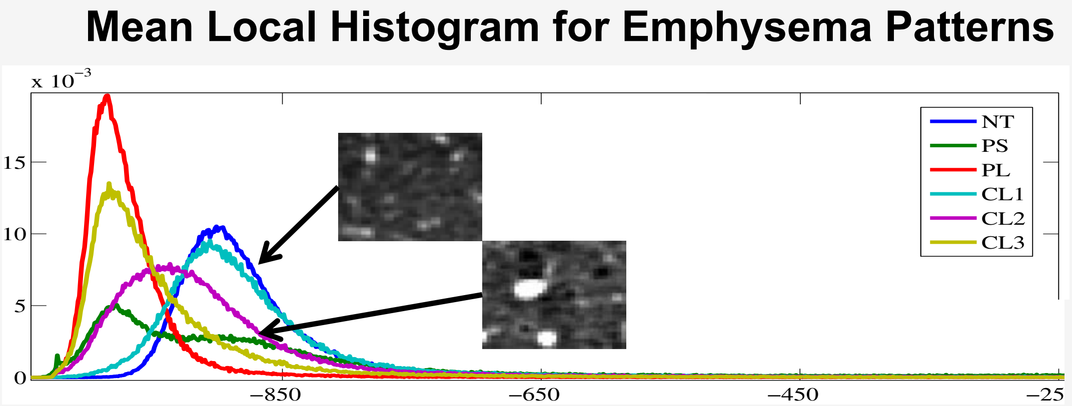

NT: Normal (non emphysema)
PS: Paraseptal
PL: Panlobular

CL1: Mild Centrilobular
CL2: Moderate Centrilobular
CL3: Severe Centrilobular

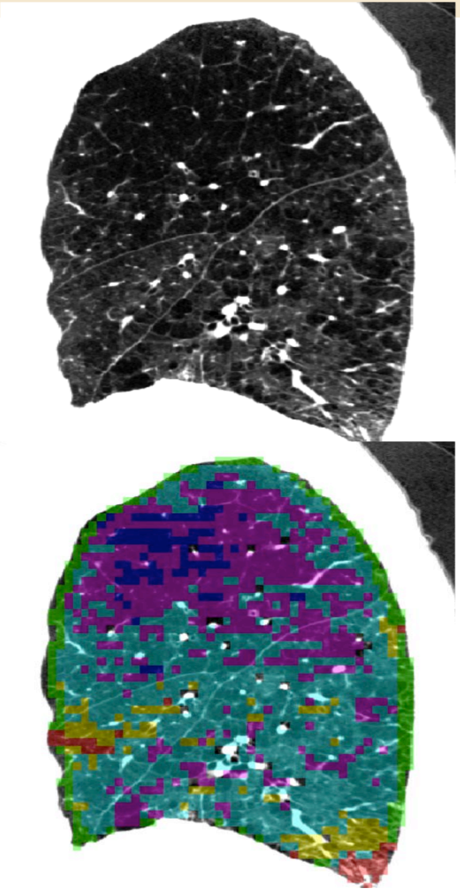

P. J. Castaldi, R. San José Estépar, et al, *Am. J. Respir. Crit. Care Med.* 2013 188(9): 1083–1090

Local Histogram Subtypes have novel GWAS

LHE Pattern	Lead SNP	Nearest Gene	Locus	Position (BP)	Effect Allele	*P* Value Meta
Normal	rs17486278	*CHRNA5*	15q25	78867482	A	8.3×10^{-13}
	rs138641402	*HHIP*	4q31	145445779	A	1.7×10^{-9}
	rs1690789	*TGFB2*	1q41	218698027	C	2.9×10^{-8}
	rs17368659	*MMP12*	11q22	102742761	G	1.1×10^{-8}
Moderate centrilobular	rs114205691	*CHRNA3*	15q25	78901113	C	3.1×10^{-13}
	rs56113850	*CYP2A6*	19q13	41353107	T	1.3×10^{-9}
	rs17368582	*MMP12*	11q22	102738075	G	2.7×10^{-9}
	rs1690789	*TGFB2*	1q41	218698027	C	7.9×10^{-9}
Severe centrilobular	rs9788721	*AGPHD1*	15q25	78802869	T	1.8×10^{-13}
	rs379123	*MYO1D*	17q11	30891814	T	1.5×10^{-8}
Panlobular	rs11852372	*AGPHD1*	15q25	78801394	A	1.5×10^{-10}
	rs9590614	*VWA8*	13q14	42175588	G	1.1×10^{-8}

- Novel associations within genes associated with cell migration (*MYO1D)* and cell signaling (*VWA8)*.
- GWAS observed at previously established COPD-associated loci
  - 14q31 (nearby gene *HHIP)*, 15q25(*CHRNA3/5/IREB2)*, 11q22 (*MMP12*), and 19q13 (*CYP2D6)*.

Castaldi et al, AJRCCM, 2013

Emphysema Subtypes and Lung Cancer

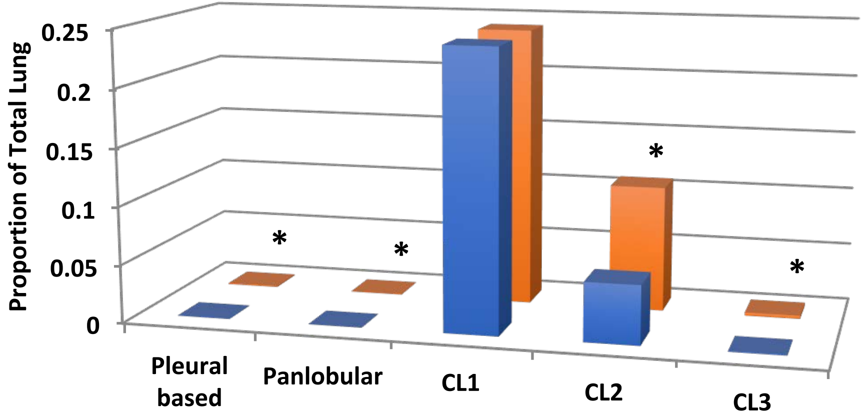

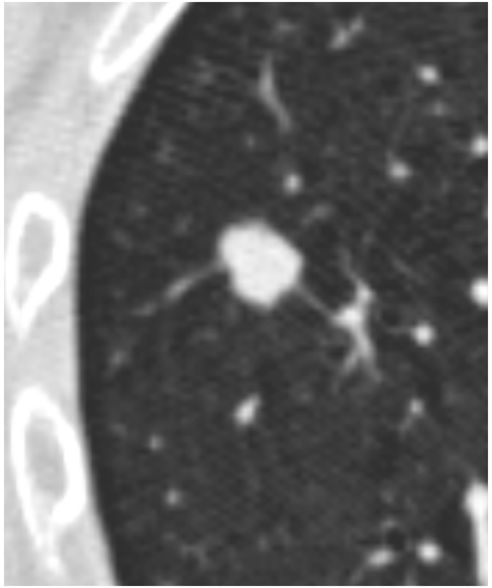

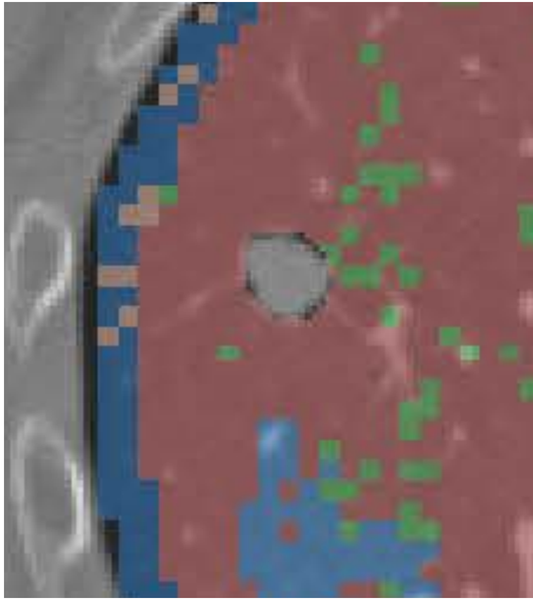

Kinsey CM, *ATS*; 2016

Lung Cancer Risk by Emphysema Subtype

Lung Parenchymal Feature	OR	CI	P value
%LAA -950 (density threshold alone)	1.01	[0.99, 1.02]	0.146
Mild centrilobular (CL1)	0.26	[0.17, 1.61]	0.263
Moderate centrilobular (CL2)	**2.41**	**[1.09, 5.32]**	**0.029**
Severe centrilobular (CL3)	6.12	[0.97, 38.6]	0.054
Panlobular (PL)	4.99	[0.23, 108.8]	0.306
Pleural-based (PB)	13.4	[0.00, 1137]	0.713

Each model includes one of the above lung parenchymal features and is adjusted for age, gender, pack years, and airflow obstruction

With the exception of %LAA-950, all morphologies were measured by the LH method at the level of the secondary pulmonary lobule.

1

Kinsey CM, *ATS*; 2016

Interstitial Lung Abnormalities

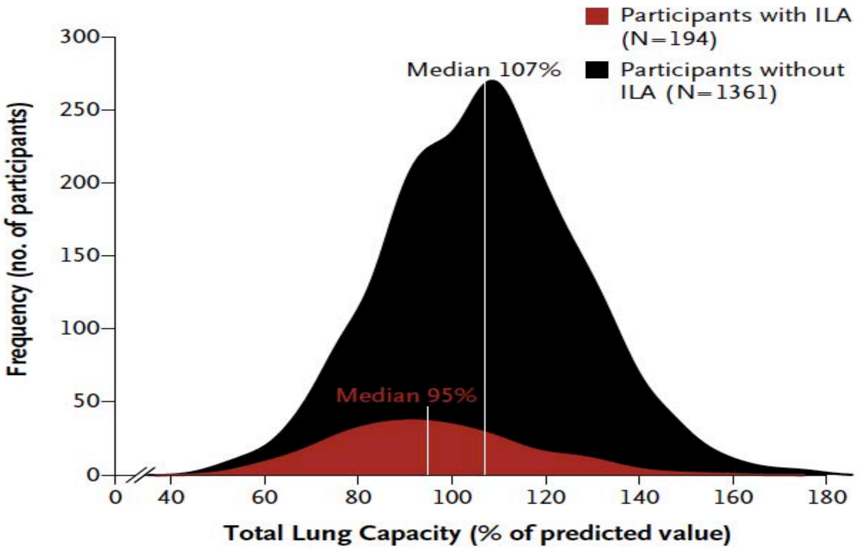

The NEW ENGLAND JOURNAL of MEDICINE

ESTABLISHED IN 1812 MARCH 10, 2011 VOL. 364 NO. 10

Lung Volumes and Emphysema in Smokers with Interstitial Lung Abnormalities

George R. Washko, M.D., M.M.Sc., Gary M. Hunninghake, M.D., M.P.H., Isis E. Fernandez, M.D., Mizuki Nishino, M.D., Yuka Okajima, M.D., Tsuneo Yamashiro, M.D., James C. Ross, M.S., Raúl San José Estépar, Ph.D., David A. Lynch, M.D., John M. Brehm, M.D., M.P.H., Katherine P. Andriole, Ph.D., Alejandro A. Diaz, M.D., Ramin Khorasani, Ph.D., Katherine D'Aco, M.S., Frank C. Sciurba, M.D., Edwin K. Silverman, M.D., Ph.D., Hiroto Hatabu, M.D., Ph.D., and Ivan O. Rosas, M.D., for the COPDGene Investigators*

The NEW ENGLAND JOURNAL of MEDICINE

ORIGINAL ARTICLE

MUC5B Promoter Polymorphism and Interstitial Lung Abnormalities

Gary M. Hunninghake, M.D., M.P.H., Hiroto Hatabu, M.D., Ph.D., Yuka Okajima, M.D., Wei Gao, M.S., Josée Dupuis, Ph.D., Jeanne C. Latourelle, D.Sc., Mizuki Nishino, M.D., Tetsuro Araki, M.D., Oscar E. Zazueta, M.D., Sila Kurugol, Ph.D., James C. Ross, M.S., Raúl San José Estépar, Ph.D., Elissa Murphy, M.S., Mark P. Steele, M.D., James E. Loyd, M.D., Marvin I. Schwarz, M.D., Tasha E. Fingerlin, Ph.D., Ivan O. Rosas, M.D., George R. Washko, M.D., George T. O'Connor, M.D., and David A. Schwartz, M.D.

Local Histogram with Interstitial Patterns

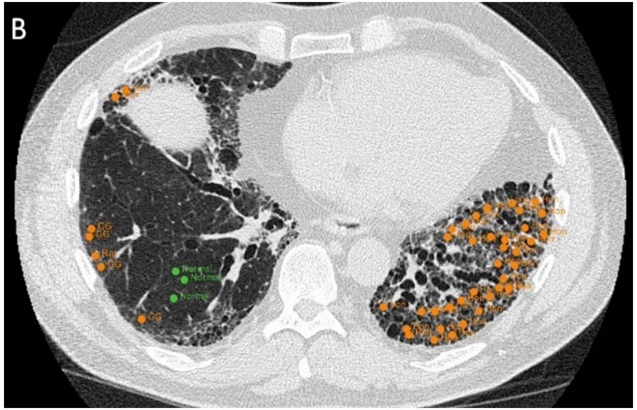

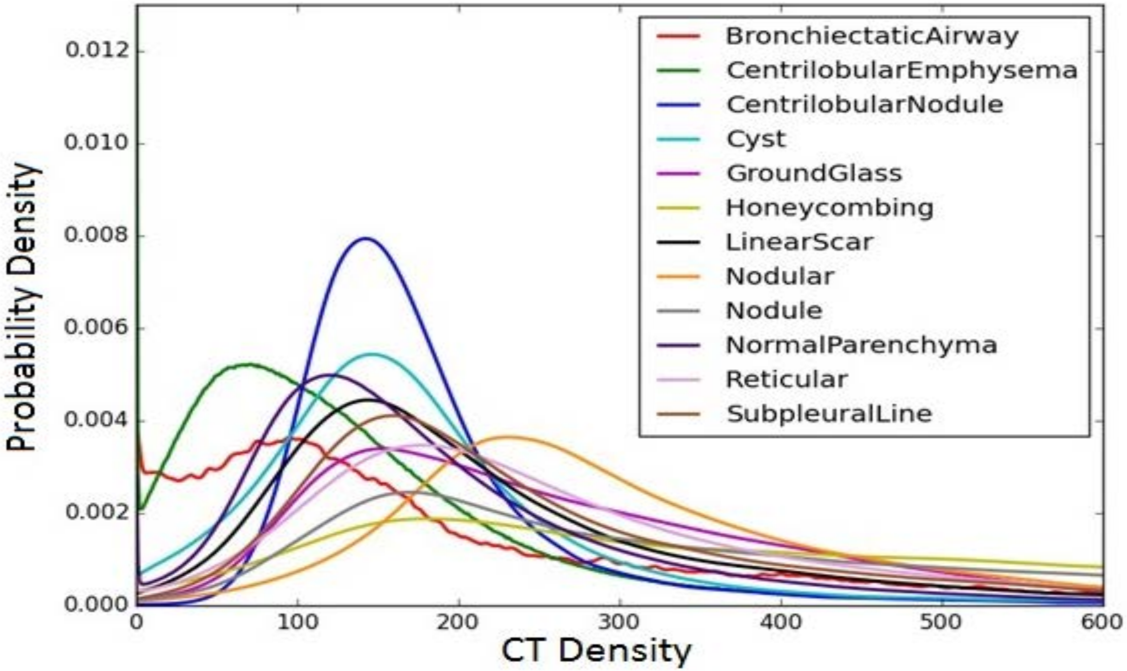

Ash SY, Harmouche R, *Academic Radiology* 2017;24

Detection of ILA matches visual diagnosis

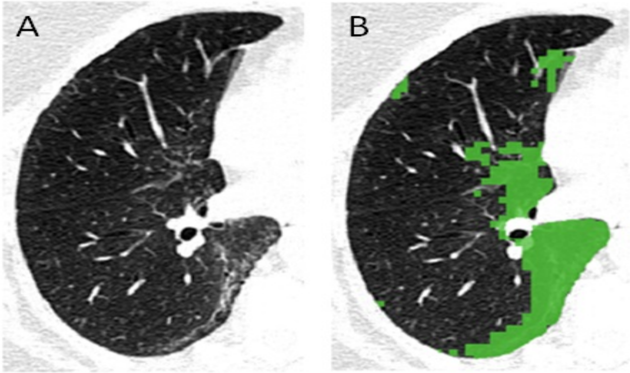

AUC 0.82 for the detection of visually defined interstitial lung abnormalities

AUC 0.89 for the detection of visually defined fibrotic parenchymal abnormalities

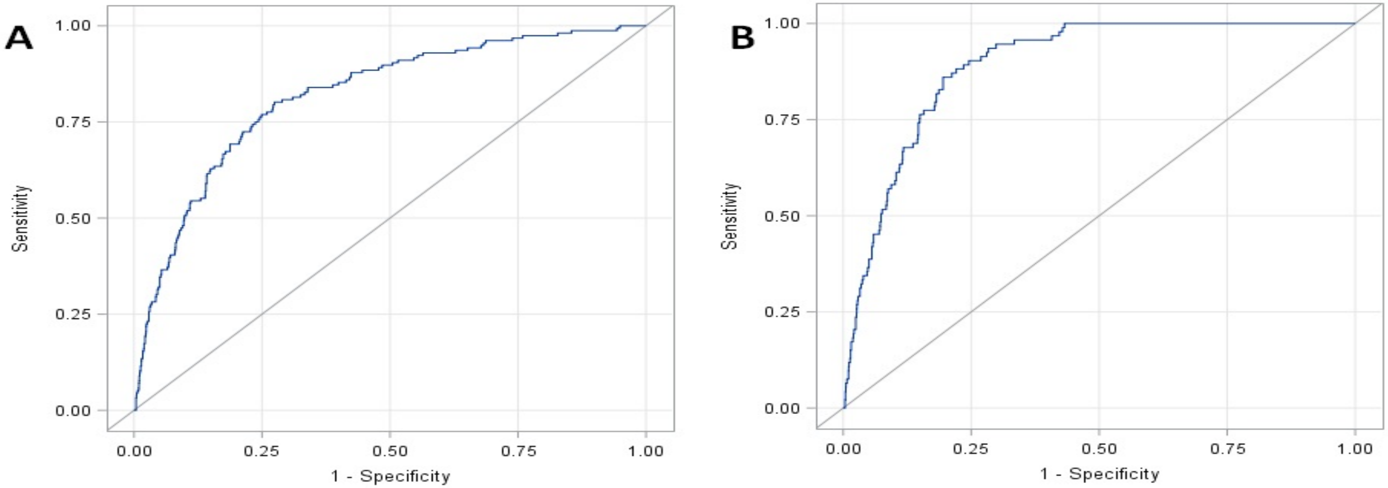

Ash SY, Harmouche R, *Academic Radiology* 2017;24

Susceptibility without visual ILA

Adjusted				
All Participants	**Change per 5% Increase in Interstitial Features**	CI	p	**All Participants**
FEV1%	-2·65	-3·15, -2·14	<0·001	
FVC%	-2·47	-2.88, -2.06	<0·001	
FEV1/FVC	-0·004	-0·007, -0.001	0·005	
SGRQ	1·36	0·92, 1·81	<0·001	
No ILA (0 only)				**Without Visual ILA**
FEV1%	-4·83	-5·78, -3·89	<0·001	
FVC%	-4·09	-4·85, -3·32	<0·001	
FEV1/FVC	-0·010	-0·016, -0·005	<0·001	
SGRQ	0·806	-0·027, 1·639	0·058	

Ash, *Chest* 2017

Mortality and Interstitial Features

	Hazard Ratio* (5% Absolute increase of ILA Features)	CI	p
All participants	1.29	1.21, 1.38	<0.001
Subgroup A – Those without ILA	1.27	1.16, 1.39	<0.001
Subgroup B – Those without ILA and without indeterminate findings	1.20	1.02, 1.42	0.031
Subgroup C – Those with normal spirometry	1.25	1.07, 1.46	0.004
Subgroup D – Those without chronic dyspnea or bronchitis	1.26	1.11, 1.44	0.001

Ash, *Chest* 2017

Parenchymal Subtyping Predicts Mortality

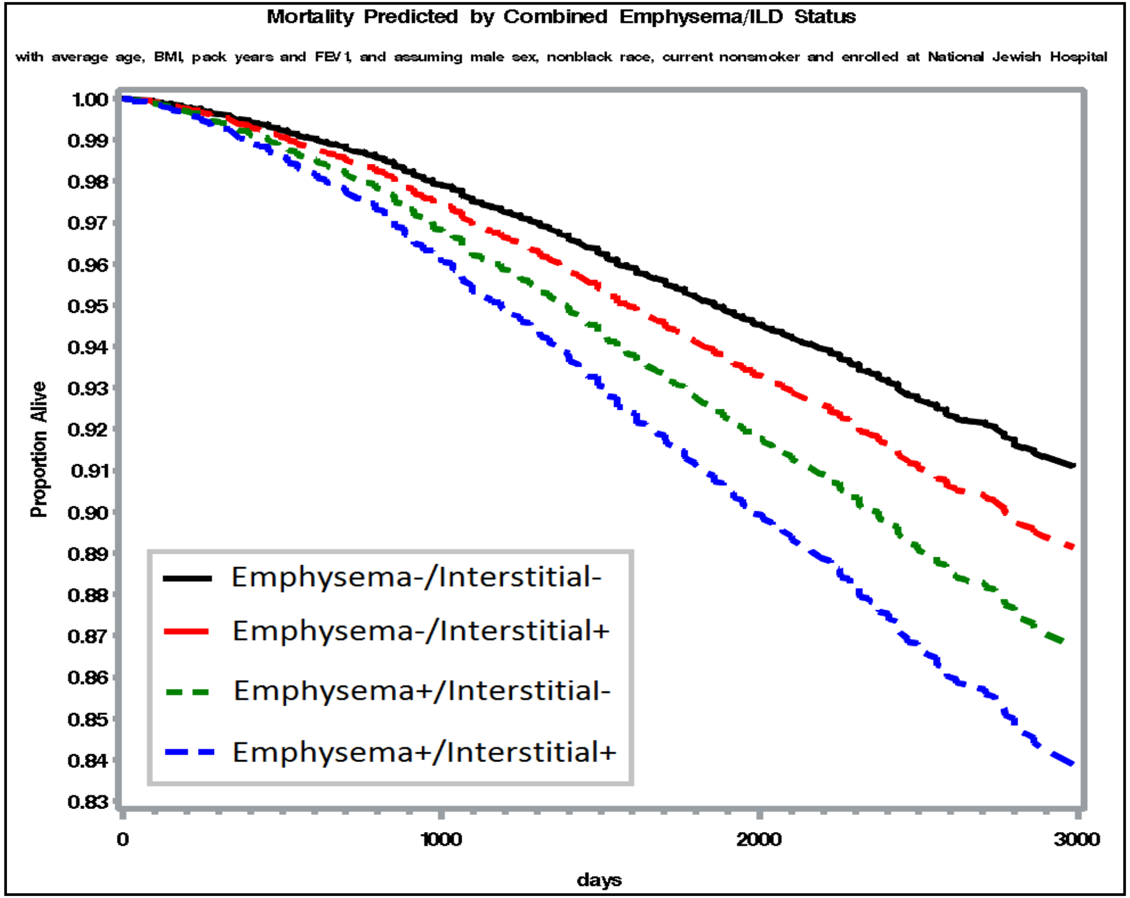

Ash, *Radiology* 2018

The AI Revolution: A new paradigm?

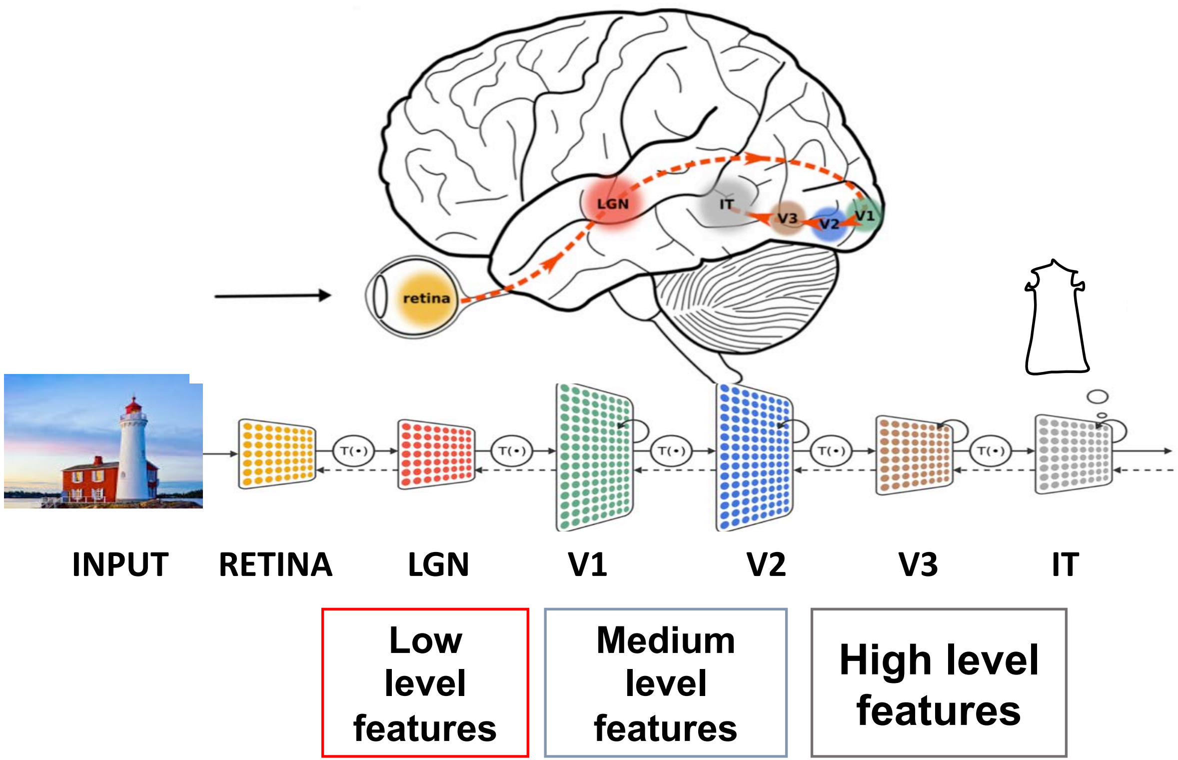

Direct Regression of Outcomes

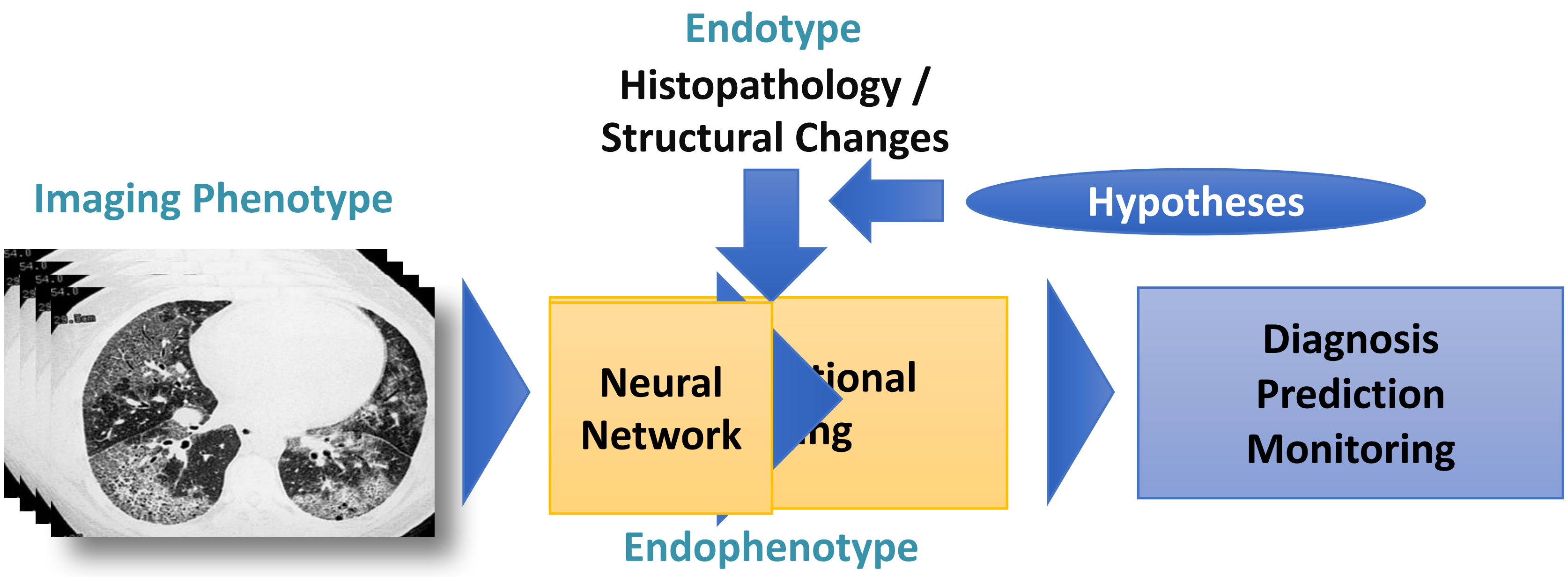

ILA subtyping with Deep Learning

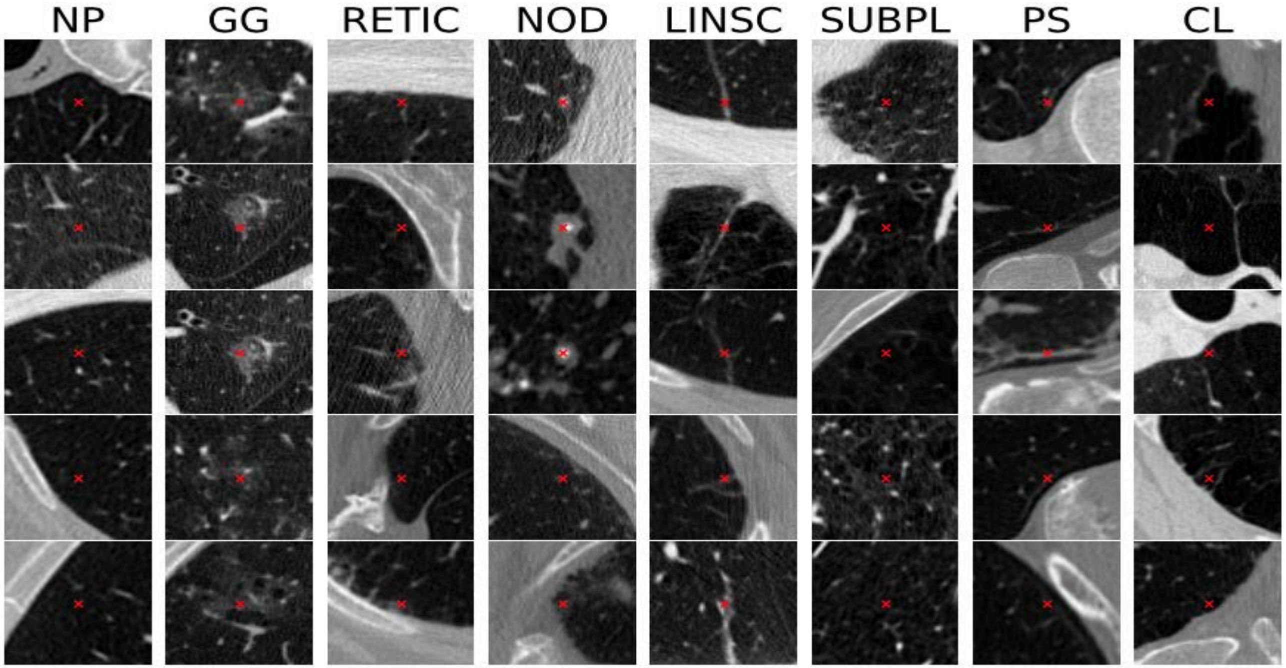

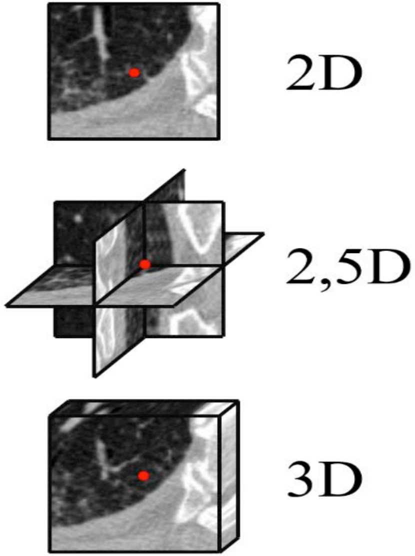

Ensemble of Convolutional Neural Networks

BCNN^{2D}	MSTAGE-CNN^{2D}	MCONTEXT-CNN^{2D}	BCNN$^{2.5D}$	MSTAGE-CNN$^{2.5D}$	BCNN^{3D}	MSTAGE-CNN^{3D}
Input: 48x48	***Input***: 48x48	***Input***: 48x48	***Input***: 3x48x48	***Input***: 3x48x48	***Input***: 48x48x7	***Input***: 48x48x7
Conv: 48@3x3	Conv:48@3x3	Conv: 48@3x3	Conv: 48@3x3	Conv:48@3x3	Conv: 48@3x3x2	Conv:48@3x3x2
Conv: 48@3x3	Conv: 48@3x3	Conv: 48@3x3	Conv: 48@3x3	Conv: 48@3x3	Conv: 48@3x3x2	Conv: 48@3x3x2
MaxPool:2x2	MaxPool:2x2	MaxPool:2x2	MaxPool:2x2	MaxPool:2x2	MaxPool:2x2x1	MaxPool:2x2x1
BatchNorm	BatchNorm	BatchNorm	BatchNorm	BatchNorm	BatchNorm	BatchNorm
Conv:48@3x3	Conv:48@3x3	Conv:48@3x3	Conv:48@3x3	Conv:48@3x3	Conv:48@3x3x2	Conv:48@3x3x2
Conv:48@3x3	Conv:48@3x3	Conv:48@3x3	Conv:48@3x3	Conv:48@3x3	Conv:48@3x3x2	Conv:48@3x3x2
MaxPool:2x2	MaxPool:2x2	MaxPool:2x2	MaxPool:2x2	MaxPool:2x2	MaxPool:2x2x1	MaxPool:2x2x1
BatchNorm	BatchNorm	BatchNorm	BatchNorm	BatchNorm	BatchNorm	BatchNorm
FC: 64	FC: 64	FC: 64	FC: 64	FC: 64	FC: 128	FC: 64
	MaxPool: 6x6	***Input***: 64x64		MaxPool: 6x6		MaxPool: 6x6x1
	BatchNorm	Conv: 48@3x3		BatchNorm		BatchNorm
	FC: 64	Conv: 48@3x3		FC: 64		FC: 64
		MaxPool:2x2				
		BatchNorm				
		Conv:48@3x3				
		Conv:48@3x3				
		MaxPool:2x2				
		BatchNorm				
		FC: 64				
	Concat: 128	Concat: 128		Concat: 128		Concat: 128
FC: 112	FC: 112	FC: 112	FC: 112	FC: 112	FC: 112	FC: 112
Softmax: 8	Softmax: 8	Softmax: 8	Softmax: 8	Softmax: 8	Softmax: 8	Softmax: 8

Bermejo, Scientific Reports, 2018, under review

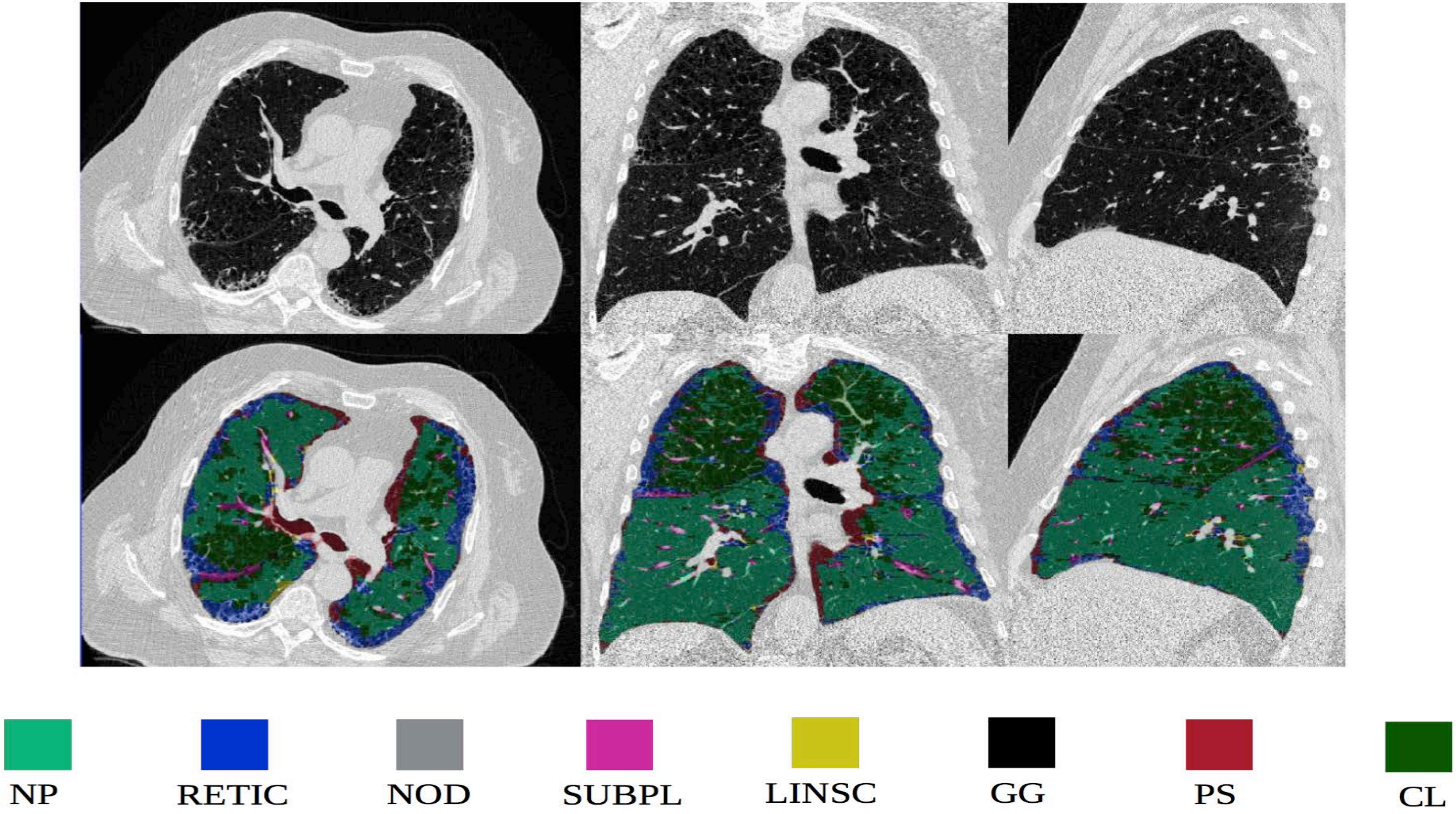
NP
RETIC
NOD
SUBPL
LINSC
GG
PS
CL

Ensemble stabilize performance

- Training in 37,424 locations
- Testing in 36,336 locations

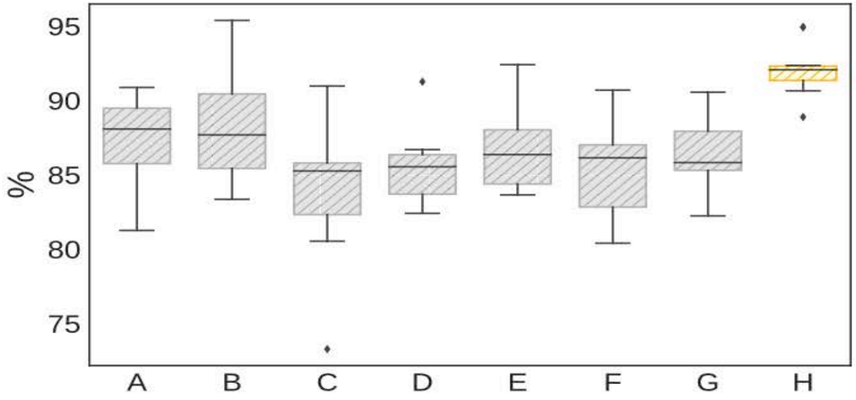

Sensitivity

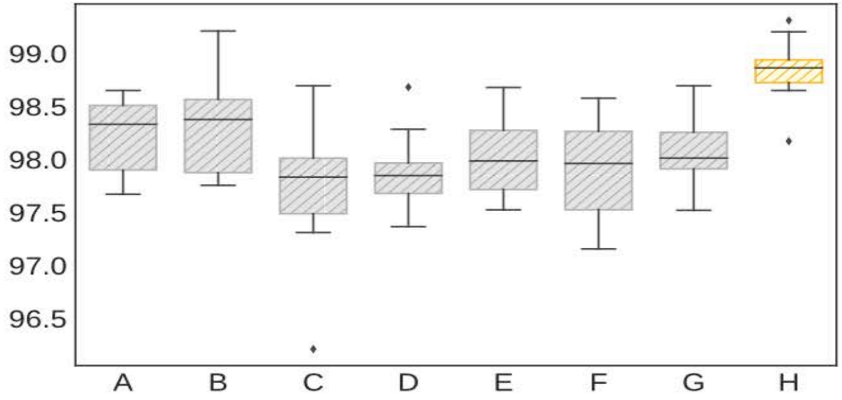

Specificity

A: $BCNN^{2D}$ B: $MSTAGE-CNN^{2D}$ C: $MCONTEXT-CNN^{2D}$ D: $BCNN^{3D}$

E: $MSTAGE-CNN^{3D}$ F: $BCNN^{2.5D}$ G: $MSTAGE-CNN^{2.5D}$ H: Ensemble

Comparison with other architectures

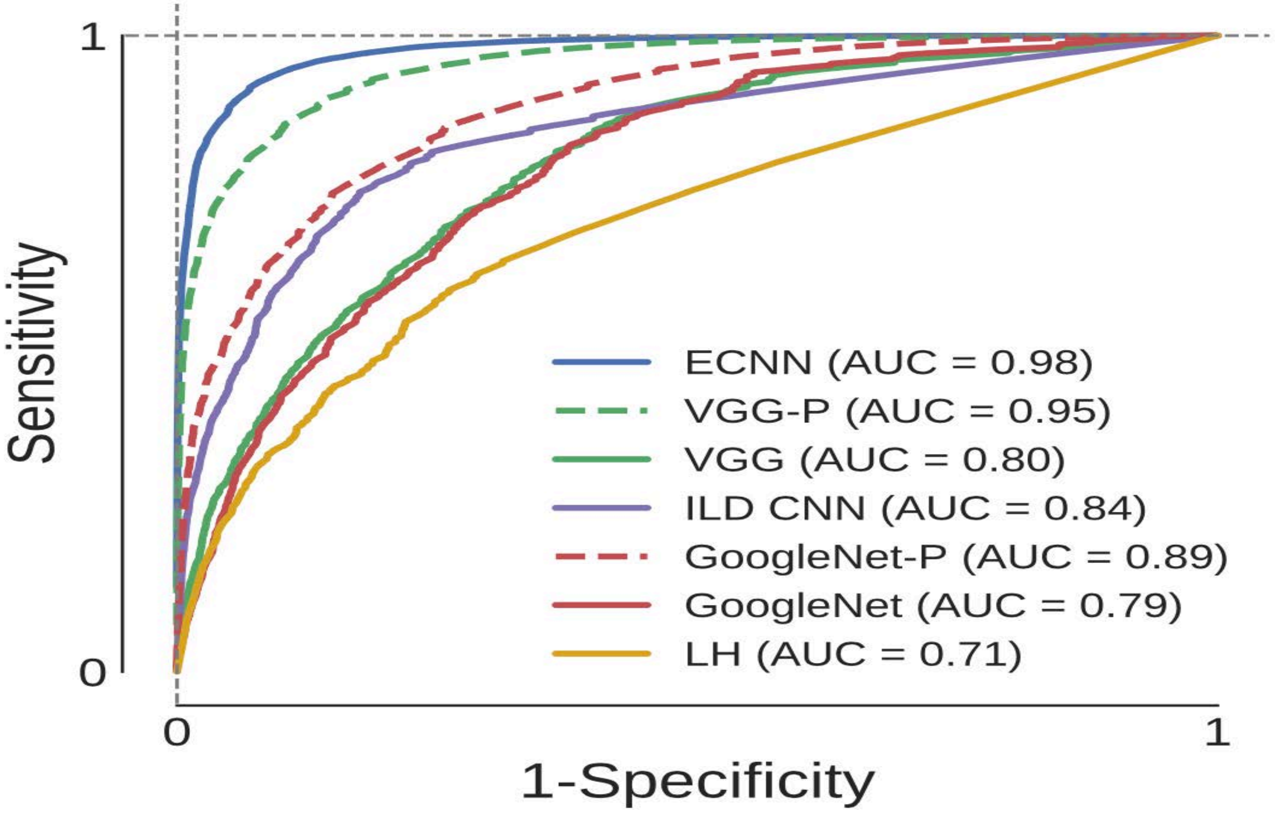

Reconstruction Stability

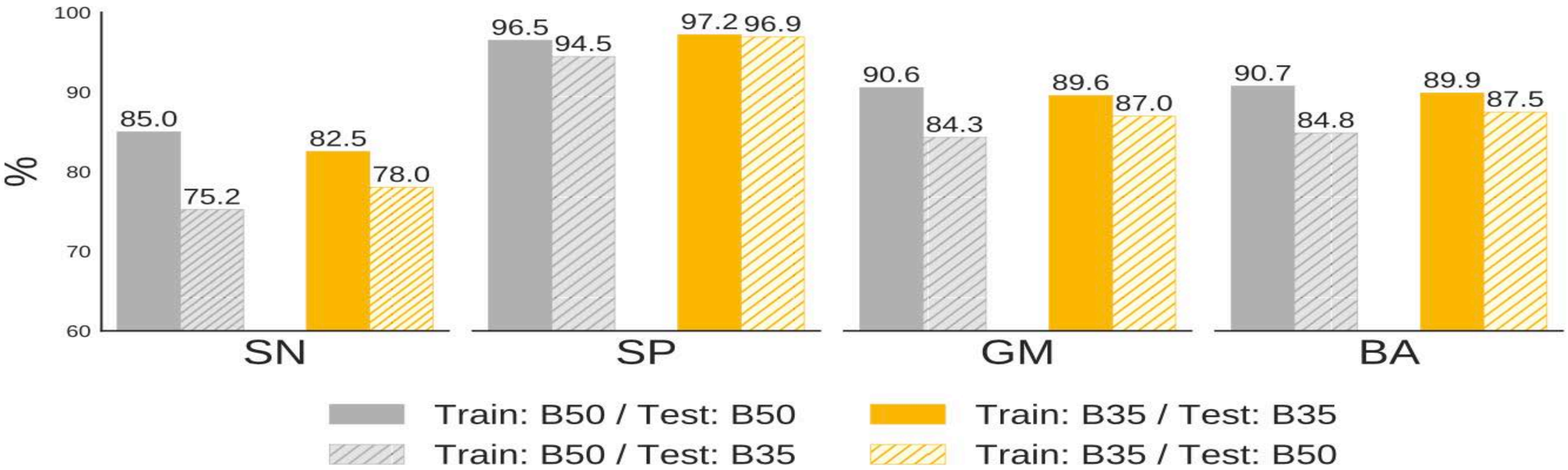

Direct Biomarker Regression

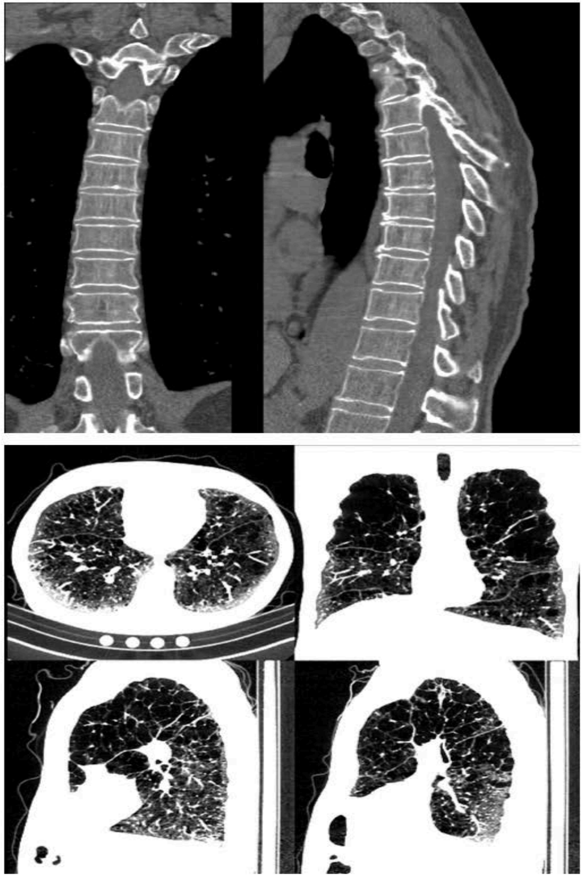

Bone Mineral Density

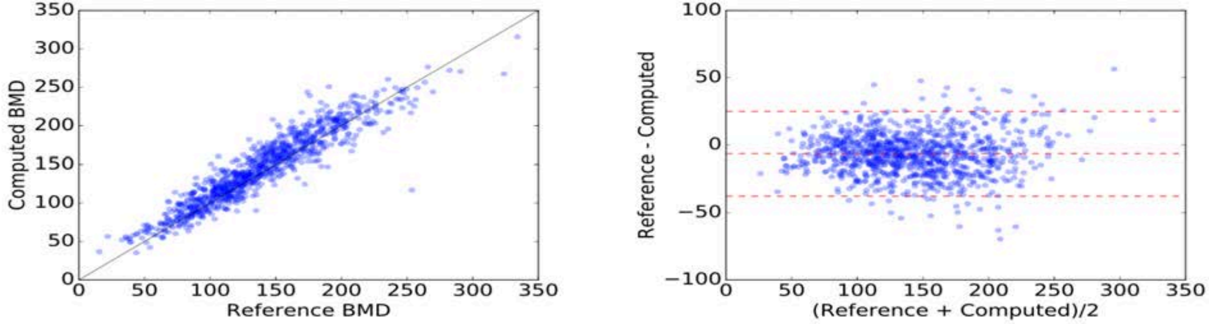

Emphysema Score

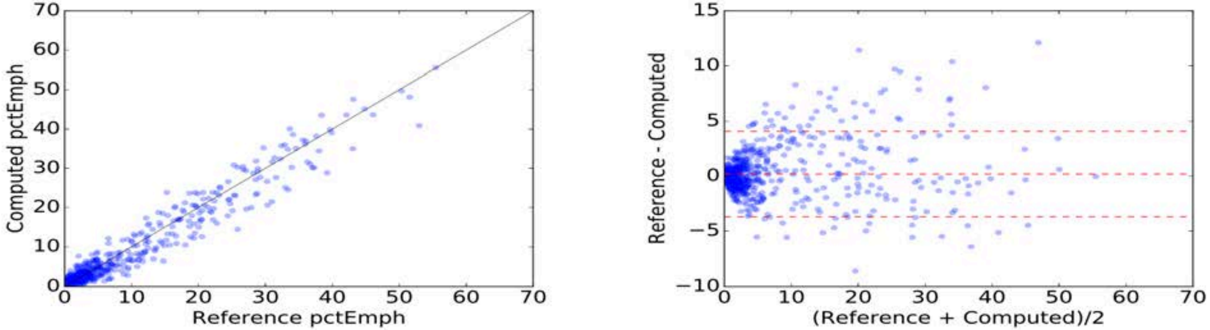

González G et al, SPIE 2018

Emphysema Scoring From X-Ray

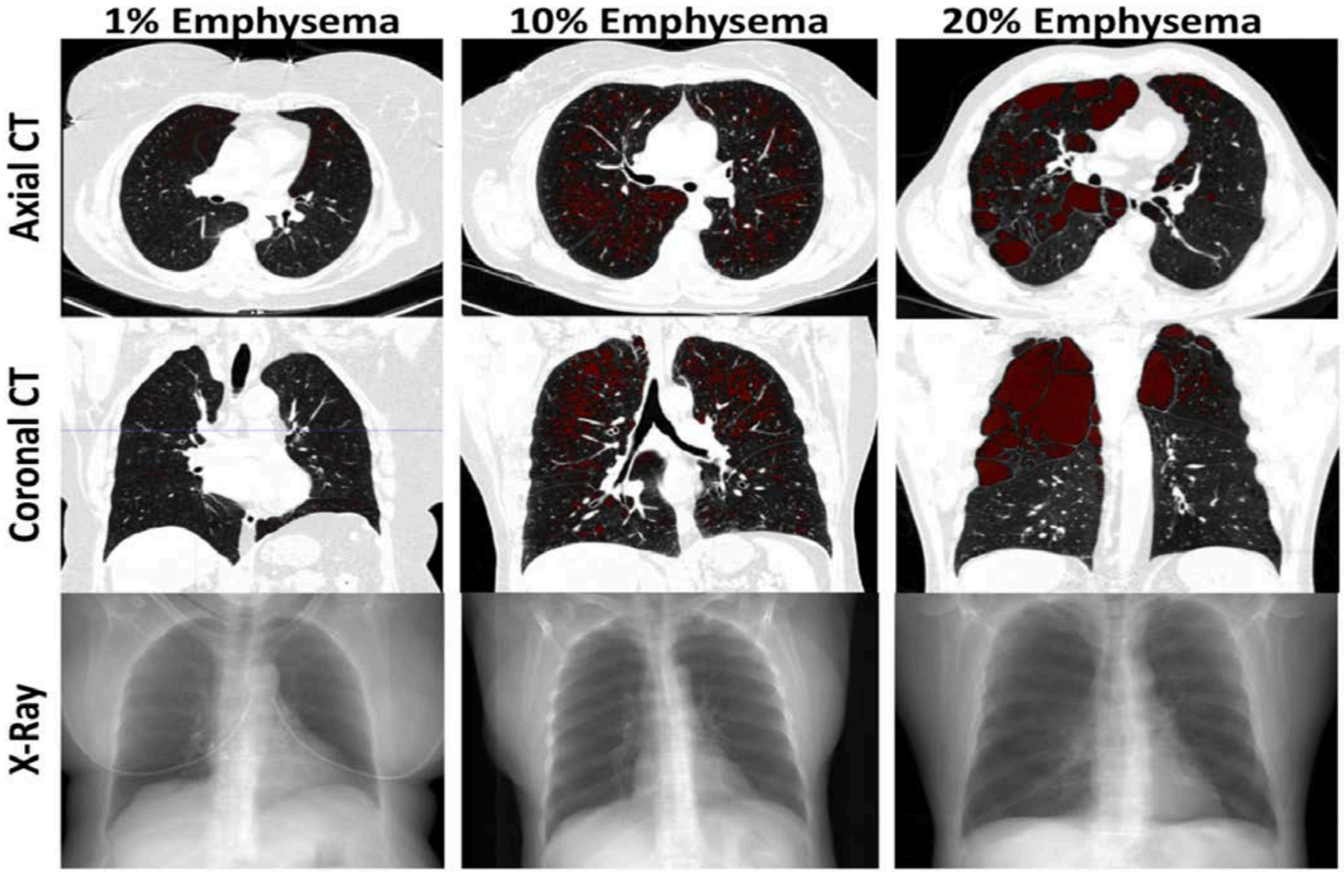

Iturrioz, ISBI 2018

Emphysema Scoring From X-Ray

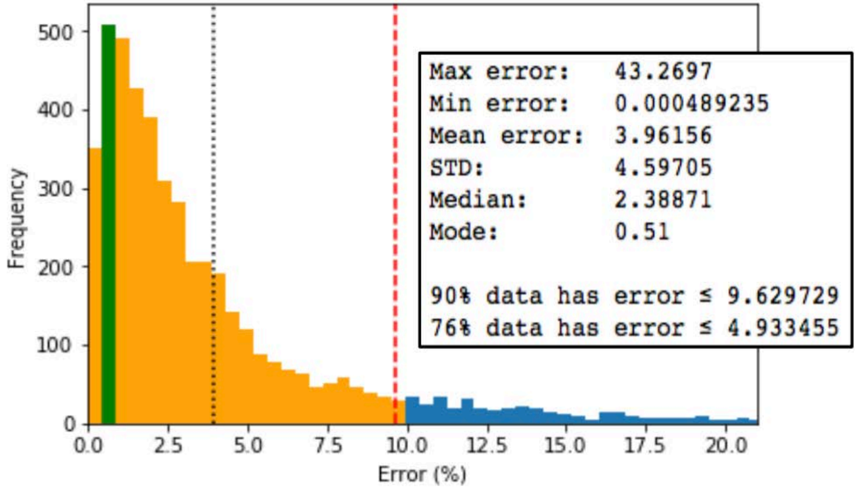

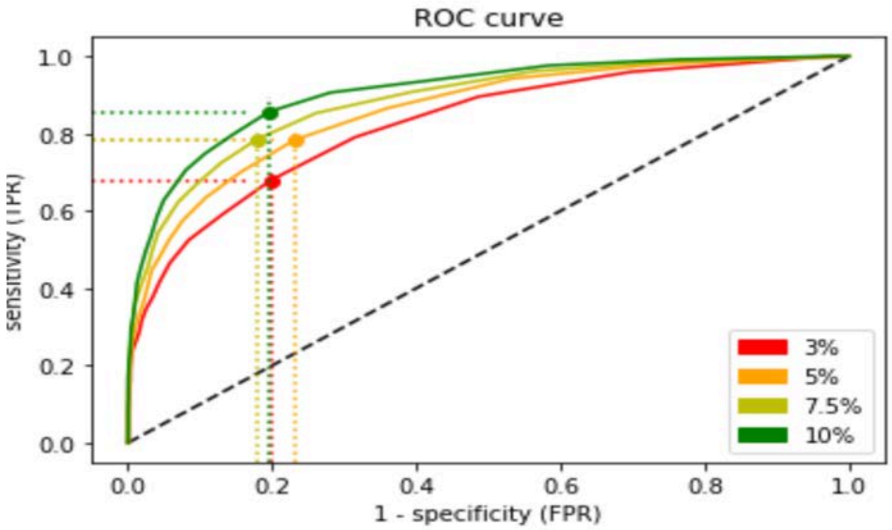

Iturrioz, ISBI 2018

Artificial Intelligence and Integral Diagnosis

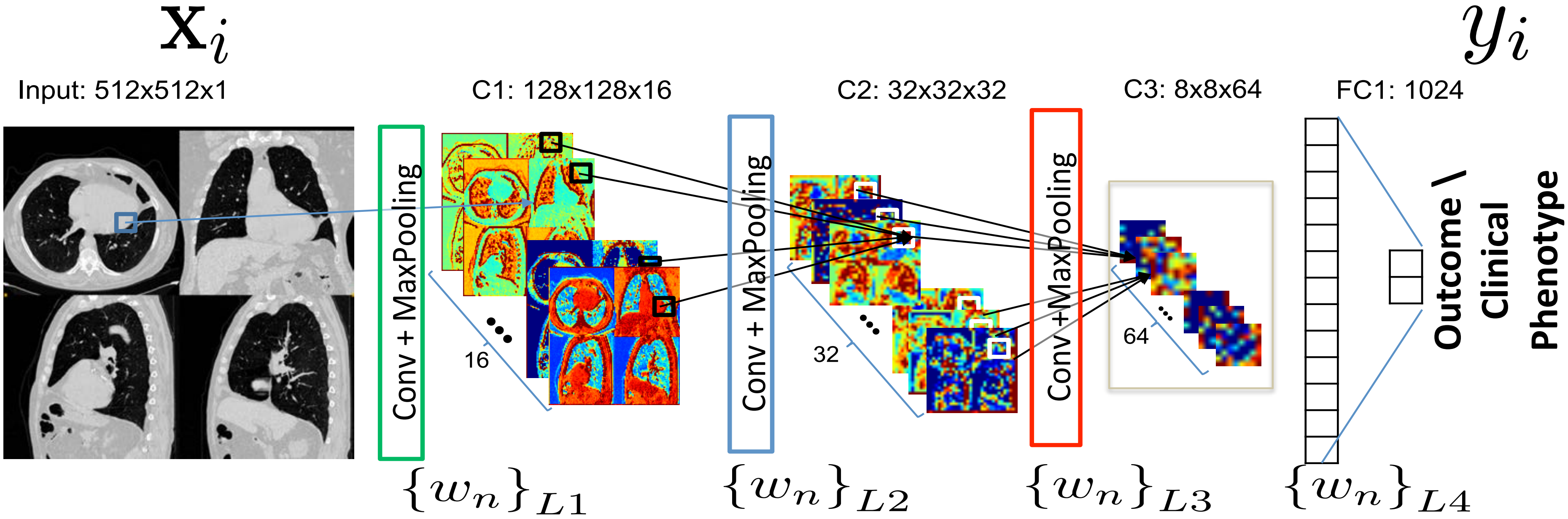

Deep Learning Performance for COPD Assessment

	COPDGene		Replication
	Reconstruction Kernel		ECLIPSE
	STD (n=1,000)	**SHARP (n=1,000)**	**(n=1,547)**
FEV1 (r coef.)	0.735 [0.705 - 0.762]	0.735 [0.705 – 0.762]	0.64 [0.542 - 0.756]
GOLD Stage (Accuracy)	51.2% / 74.7%	52.0% / 73.8%	29.4% / 74.6%
ARD AUC	0.633 [0.602 - 0.663]	0.627 [0.597 – 0.658]	0.55 [0.51 - 0.62]
Mortality AUC	0.72 [0.6 - 0.78]	0.709 [0.58 – 0.737]	0.6 [0.52 - 0.71]

González Serrano G, *Am J Respir Crit Care Med,* 2017

Conclusions

- Parenchymal Injury is a crucial marker of the host inflammatory response to tobacco injury.
- Quantitative assessment of parenchymal injury (emphysema and ILD) is clinically relevant even in asymptomatic.
- Artificial Intelligence may offer a new paradigm for image-based biomarker computation
  - Quality and through testing are a key factor for translation

Acknowledgements

Applied Chest Imaging Laboratory

- Carrie Aaron
- Samuel Ash
- Carolyn Come
- Alejandro Diaz
- Ruben San Jose
- Rola Harmouche
- Stefanie Mason
- Pietro Nardelli
- Yuka Okajima
- Jorge Onieva
- Nick Rahagi
- James Ross
- Gonzalo Vegas Sanchez-Ferrero
- German Gonzalez Serrano
- George Washko

- **NHLBI**
  - R01HL116931
  - R01HL116473
  - COPDGene Study
- COPDGene Investigators

BRIGHAM HEALTH

BRIGHAM AND WOMEN'S HOSPITAL

Thank you

rsanjose@bwh.harvard.edu

HARVARD MEDICAL SCHOOL TEACHING HOSPITAL